Prefrontal Cortex transcranial Direct Current Stimulation via a Combined High Definition and Conventional Electrode Montage: A FEM modeling studying

Dennis Q. Truong, Abhishek Datta, Jiansong Xu, Felipe Fregni, and Marom Bikson

Abstract— **The prefrontal cortex (PFC) is a common target during transcranial Direct Current Stimulation (tDCS) due to its functional implication in a range of normal cognitive function and disease. Clinical studies use a heuristic montage design with a large active electrode over the target. Using a standard MRI-derived Finite Element model, we simulated PFC current flow generated with a combination of High-Definition and conventional tDCS electrodes. Specifically considered are bi-frontal HD electrodes with a conventional electrode return. We report that the position of both the HD electrode and return electrode determined overall brain current flow including across PFC. These "2x1-Hybrid" montages may be considered for future efforts using tDCS in clinical and cognitive studies.**

I. Introduction

Transcranial Direct Current Stimulation (tDCS) has been and is being used in a broad spectrum of experiments, ranging from basic cognitive research to clinical trials. tDCS involves passage of low-intensity current through electrodes on the scalp to produce weak electric fields in the brain that lead to neuromodulation and plasticity. The flexibility of tDCS and its customization to a broad range of applications stems from the ability to shape the flow of brain current by selecting the electrode montage. One region in particular, the prefrontal cortex (PFC), has been implicated in affecting a range of normal brain processes and pathology, and so has been nominally targeted in tDCS research. Clinical studies have suggested conditions such as depression, alcohol cravings, and working memory can benefit from tDCS of the PFC [1]–[3].

The selection of a tDCS montage for PFC stimulation has typically followed a basic "rule-of-thumb" approach using conventional tDCS sponge electrodes (~25 cm^2 pads) where the active electrode (anode or cathode) is placed over PFC and the return (cathode or anode) over of another brain region. Yet, several modeling studies have shown that brain current flow during tDCS may be complex and idiosyncratic. Depending on electrode montage, peak brain current flow may in fact be between rather than under the electrodes [4]–[7]. The position of the return electrode will influence overall current flow including under the active electrode [8]. Therefore, the influence of the return electrode cannot be selectively ignored.

Attempts to focalize tDCS include decreasing the size of the active sponge electrode, while increasing the size of the return electrode [9], [10]. The use of smaller High-Definition (HD) electrodes [11] has allowed stimulation with multiple electrodes in optimized configurations [12] including the 4x1-Ring [4]. Here, we simulate PFC current flow generated using a combination of two frontal HD electrodes and one conventional return electrode. Our goal was to understand and optimize bilaterally symmetric PFC and general brain current flow using this relatively simple to implement "2x1-Hybrid" configuration.

II. Methods

Finite Element (FE) models were generated and solved for a variety of montages based on the International 10-10 system for electroencephalogram (EEG) electrode placement. In each of these montages, two HD electrodes are active and a single 5x5 pad is the return. Specifically, the montages modeled were: F3 and F4 active, neck return; F3 and F4 active, Pz return; F3 and F4 active, Oz/POz return; AF3 and AF4 active, Oz/POz return; Fp1 and Fp2 active, Oz/POz return; Fp1 and Fp2 active, Cz return. These models were derived from the same T1 magnetic resonance imaging (MRI) scan with a spatial resolution of 1x1x1 mm of a healthy adult male. These models followed electrostatic volume conductor assumptions. With the exception of electrode positioning, a common method was shared by the models that can be delineated into two primary phases: the model construction and the model solution.

A. Model Construction

The geometry of the volume conductors were originally derived from a high resolution 3T MRI scan ($1mm^3$). Initially, the MRI scan was automatically segmented using Statistical Parametric Mapping (SPM8) software. This automated segmentation software was used to delineate six different tissues within the MRI scan: skin, bone, cerebral spinal fluid (CSF), gray matter, white matter, and air. The automatic segmentation; however, was not perfect. Spatial aliasing problems existed in thin layers such as the CSF and in parts of the gray matter. This required manual correction

*Research supported by The Wallace H Coulter Foundation

D.Q. Truong, A. Datta, and M. Bikson are with the Department of Biomedical Engineering, The City College of the City University of New York, New York, NY 10031 USA (phone: 212-650-8876; fax: 212-650-6727; e-mail: dtruong01@ccny.cuny.edu).

J. Xu is with the Department of Psychiatry, Yale Medical School, New Haven, CT 06519 USA. (e-mail: :jiansong.xu@yale.edu).

F. Fregni is with the Berenson-Allen Center for Noninvasive Brain Stimulation, Beth Israel Deaconess Medical Center, Harvard Medical School, Boston, MA 02215 USA (e-mail: ffregni@bidmc.harvard.edu).

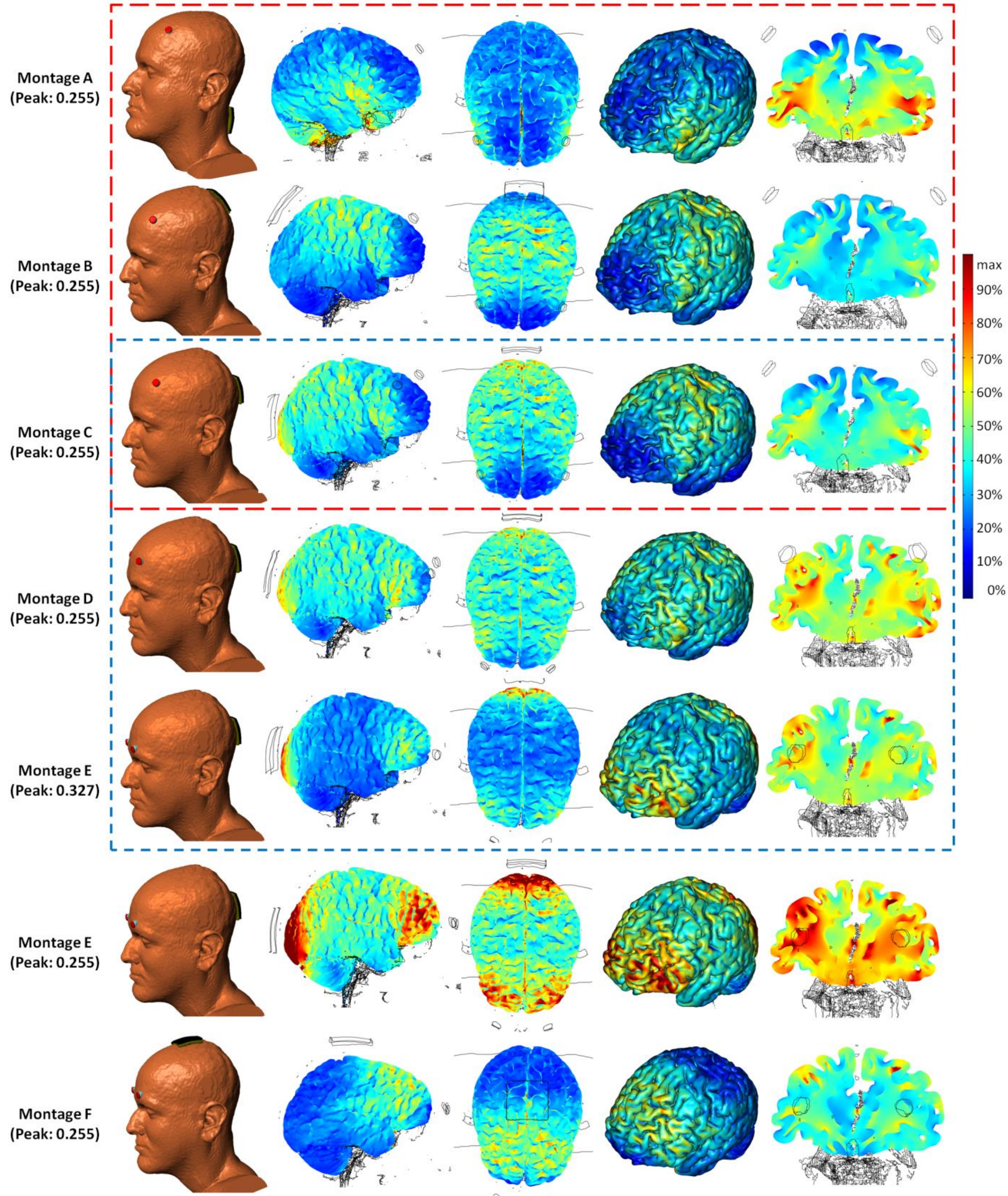

Figure 1: Electric field generated during tDCS using six hybrid (HD plus conventional electrode) montages. From left to right, the columns contain images of the electrode placement on the skin, peak electric field viewed from the right hemisphere, peak electric field viewed over the dorsal surface, peak electric field viewed from the left hemisphere with additional lighting to display morphology, and a coronal slice under F3-F4. The dashed red box represents montages in which the active electrode is fixed. The dashed blue box represents the montages in which the return electrode is fixed. Montages A, B, C, D, E, and F represent the following: F3 and F4 active, neck return; F3 and F4 active, Pz return; F3 and F4 active, Oz/POz return; AF3 and AF4 active, Oz/POz return; Fp1 and Fp2 active, Oz/POz return; Fp1 and Fp2 active, Cz return.

to patch small holes as well as to resolve additional detail in anatomical features such as the cortical surface. Additional smoothing was applied to the surface of skin via Gaussian filters. This manual correction, filtering, and subsequent volume meshing was performed using ScanIP+Fe (SIMPLEWARE LTD., UK).

Prior to meshing; however, the stimulation electrodes, pads, and gel had to be modeled, imported into the segmentation model, and positioned upon the head. This was accomplished using a variety of tools, starting with the computer aided design (CAD) program, Solidworks (DS SolidWorks, MA). The sponge pad was created by sketching a curved rectangular profile in one plane and sweeping this sketch in an orthogonal plane. This was done to create a pad that resembles a conventional 5x5 cm pad with a thickness of about 1 cm. This process was then repeated to create a 5x5 cm electrode that would fit directly on top of the aforementioned pad. The HD electrodes and gels were created in similar fashion by extruding a 4 mm radius circle to form a 4 mm thick disk. These CAD models were then exported as a Standard Tessellation Language (STL) file and imported into ScanCAD (SIMPLEWARE LTD., UK) along with the segmentation model. Here, the CAD models were placed upon the head and converted into a segmentation mask.

The following “2x1-Hybrid” montages were evaluated:

- Montage A: HD electrodes at F3 and F4, return pad centered on the neck.
- Montage B: HD electrodes at F3 and F4, return pad centered at Pz
- Montage C: HD electrodes at F3 and F4, return pad centered between Oz/POz.
- Montage D: HD electrodes at AF3 and AF4, return pad centered between Oz/POz.
- Montage E: HD electrodes at Fp1 and Fp2, return pad centered between Oz/POz.
- Montage F: HD electrodes at Fp1 and Fp2, return pad centered at Cz.

The HD electrodes always have the same polarity, and the return the opposite polarity. Because of the linearity of the solution, our results can be applied for either the HD-anode/pad-cathode case or HD-cathode/pad-anode case (only electric field magnitude, not current direction, is represented). The use of “active” to describe the HD electrodes and “return” to describe the pad is thus arbitrary with current flow across the whole brain. Similarly, because of linearity the results can be extrapolated to any current intensity of DC/low-frequency AC waveform.

The completed segmentation model – head, pads, and electrodes – was then meshed in ScanIP+Fe using the adaptive tetrahedral meshing algorithm. This produced meshes with approximately 9 million quadratic elements, which correspond with about 12 million degrees of freedom.

B. Model Solution

The meshes were then imported into an FE solver (COMSOL Multiphysics 3.5a, COMSOL Inc., MA). Within the FE solver, isotropic conductivities were assigned to each subdomain – to each tissue, pad, and electrode within the mesh. These conductivities (in S/m) were assigned as follows: skin: 0.465, skull: 0.01, CSF: 1.65, gray matter: 0.276, white matter: 0.126, air: 1e-15, sponge pad: 1.4, gel: 0.3, electrode: 5.99e7. [4], [13]

Boundary conditions were then applied to the model. The surfaces of the model that were exposed to the surrounding air were assumed to be insulated. This included the surfaces at the base of the neck and shoulders where the model was truncated. Exceptions to this were the exposed surfaces of the electrodes. The surfaces of the HD electrodes were assigned to have an inward current of $1 A/m^2$ each. For 2 HD electrodes, this corresponds to $2 A/m^2$. Taking into account the area of the exposed surfaces, this corresponds to a total current injection of about 4.9e -4 A. The return electrode was also assign a separate boundary condition; it was assigned the condition of ground, i.e. V=0. All other boundaries, namely all the internal boundaries, were set as continuous.

The FE models were solved to a relative tolerance of 1e-6. The results were plotted as false color images of the electric field of the cortical surface. Like previous tDCS modeling studies [4]–[7], it is believed that membrane depolarization can be elicited when electric field peaks coincide with axon terminals or bends [14]. Based on this assumption, electric field intensity was the chosen metric for stimulation.

III. RESULTS

The location of electric field peaks varied significantly with both the position of the active and passive electrodes. By manipulating both sets of electrodes, current flow can be directed to or away from certain regions. In Fig. 1, six different hybrid montages are presented. The position of the bipolar HD electrodes at F3 and F4 are held fixed in Montages A, B, and C as the position of the return electrode is varied (dashed red line). In Montages C, D, and E the position of the return electrode is held constant at Oz/POz (dashed blue line) as the position of the bipolar HD electrodes is varied. It can be seen in each set that current flow is modulated by the combined position of the HD electrodes and return electrode.

In each montage, the resulting complex pattern of cortical current flow can be understood by consulting the figures. But several features are notable. For example, the current slips underneath the brain in Montage A as current flows towards the neck pad. Moving the return pad higher, more superior, as in Montages B and C, leads to electric field peaks on the dorsal side of the cortex.

Position of the return on Oz/POz produced significant current across occipital cortex for all HD electrode positions tested, but the overall current flow across the brain, including PFC, is different. In Montage C, peak electric field does not appear directly under the active electrodes, but rather appears between the active and the return. However, this skewing effect appears to be reduced as the active electrodes are moved further inferior and consequently further away from each other as seen in Montages D and E. In fact, in Montage E peak electric field is not between the active and return, but is rather underneath the electrodes. Electric field intensity is substantially higher in this montage and had to be plotted to a different scale. Plots of Montage E at the same scale as the other montages are included in Fig. 2 as well.

An important point, which illustrates the limits of rule-of-thumb montage design, is that effective montages can be designed in which electrode placement is not necessarily directly over the area of interest. In Montage F, the active electrodes are placed inferior of the dorsal lateral prefrontal cortex (DLPC) atop Fp1 and Fp2, while the return is placed nearby, posterior of the DLPC atop the vertex position Cz. It can be seen that peak electric field is neither directly under Fp1 and Fp2 or Cz; rather, peak electric field occurs between the electrodes reaching more of the DLPC and less of the orbitofrontal cortex.

IV. Conclusion

There is no "magic bullet" for specific modulation of only PFC; rather each montage results in specific patterns of current flow across PFC and other cortical regions. Ultimately, the most suitable montage will depend on the clinical study objectives. Having a greater variety of possible montages will allow for greater flexibility in tailoring the stimulation prescription to match these clinical needs. The 2x1-Hybrid montages evaluated here present additional alternatives for "rational" tDCS design that is still relatively straightforward to implement. Specifically: 1) Two "HD" electrodes [11] can be positioned on the forehead using a conventional EEG cap or even, for below hairline positions, adhesives; 2) The return electrode is a conventional pad positioned using a cap or straps; 3) Electrodes can be energized using a conventional 1x1 tDCS stimulator with a passive split to the HD pair, assuming reasonable impedance matching, or active control (2x1).

More complex platforms make use of additional HD electrodes for targeted [4] and automatically optimized [12] configurations. The 2x1 Hybrid represents a middle ground between traditional pads, with poor targeting, and multichannel electrode arrays, which require specialized software and hardware.

As common for modeling studies, the representation of "neuromodulation intensity" is assumed to reflect local electric field (Quasi-Uniform assumption), though consideration of directionality or explicit neuron modeling may provide additional insight. Interestingly, the use of two "lint" supra-orbital active electrodes (with an extracephalic return) dates to early clinical studies of electrosleep and cranial electrostimulation [15]–[17].

References

[1] P. S. Boggio, S. P. Rigonatti, R. B. Ribeiro, M. L. Myczkowski, M. A. Nitsche, A. Pascual-Leone, and F. Fregni, "A randomized, double-blind clinical trial on the efficacy of cortical direct current stimulation for the treatment of major depression," *The International Journal of Neuropsychopharmacology*, vol. 11, no. 2, p. 249, 2008.

[2] P. S. Boggio, N. Sultani, S. Fecteau, L. Merabet, T. Mecca, A. Pascual-Leone, A. Basaglia, and F. Fregni, "Prefrontal cortex modulation using transcranial DC stimulation reduces alcohol craving: a double-blind, sham-controlled study," *Drug and alcohol dependence*, vol. 92, no. 1–3, pp. 55–60, 2008.

[3] F. Fregni, P. S. Boggio, M. Nitsche, F. Bermpohl, A. Antal, E. Feredoes, M. A. Marcolin, S. P. Rigonatti, M. T. A. Silva, W. Paulus, and A. Pascual-Leone, "Anodal transcranial direct current stimulation of prefrontal cortex enhances working memory," *Experimental Brain Research*, vol. 166, no. 1, pp. 23–30, Jul. 2005.

[4] A. Datta, V. Bansal, J. Diaz, J. Patel, D. Reato, and M. Bikson, "Gyri-precise head model of transcranial direct current stimulation: improved spatial focality using a ring electrode versus conventional rectangular pad," *Brain Stimul*, vol. 2, no. 4, pp. 201–207, 207.e1, Oct. 2009.

[5] R. J. Sadleir, T. D. Vannorsdall, D. J. Schretlen, and B. Gordon, "Transcranial direct current stimulation (tDCS) in a realistic head model," *Neuroimage*, vol. 51, no. 4, pp. 1310–1318, 2010.

[6] T. Wagner, F. Fregni, S. Fecteau, A. Grodzinsky, M. Zahn, and A. Pascual-Leone, "Transcranial direct current stimulation: A computer-based human model study," *NeuroImage*, vol. 35, no. 3, pp. 1113–1124, Apr. 2007.

[7] P. C. Miranda, M. Lomarev, and M. Hallett, "Modeling the current distribution during transcranial direct current stimulation," *Clinical Neurophysiology*, vol. 117, no. 7, pp. 1623–1629, Jul. 2006.

[8] M. Bikson, A. Datta, A. Rahman, and J. Scaturro, "Electrode montages for tDCS and weak transcranial electrical stimulation: Role of 'return' electrode's position and size," *Clin Neurophysiol*, vol. 121, no. 12, pp. 1976–1978, Dec. 2010.

[9] M. A. Nitsche, S. Doemkes, T. Karaköse, A. Antal, D. Liebetanz, N. Lang, F. Tergau, and W. Paulus, "Shaping the effects of transcranial direct current stimulation of the human motor cortex," *J. Neurophysiol.*, vol. 97, no. 4, pp. 3109–3117, Apr. 2007.

[10] M. A. Nitsche, L. G. Cohen, E. M. Wassermann, A. Priori, N. Lang, A. Antal, W. Paulus, F. Hummel, P. S. Boggio, F. Fregni, and others, "Transcranial direct current stimulation: State of the art 2008," *Brain Stimulation*, vol. 1, no. 3, pp. 206–223, 2008.

[11] P. Minhas, V. Bansal, J. Patel, J. S. Ho, J. Diaz, A. Datta, and M. Bikson, "Electrodes for high-definition transcutaneous DC stimulation for applications in drug delivery and electrotherapy, including tDCS," *Journal of Neuroscience Methods*, vol. 190, no. 2, pp. 188–197, Jul. 2010.

[12] J. P. Dmochowski, A. Datta, M. Bikson, Y. Su, and L. C. Parra, "Optimized multi-electrode stimulation increases focality and intensity at target," *Journal of Neural Engineering*, vol. 8, p. 046011, 2011.

[13] A. Datta, J. M. Baker, M. Bikson, and J. Fridriksson, "Individualized model predicts brain current flow during transcranial direct-current stimulation treatment in responsive stroke patient," *Brain Stimulation*, vol. 4, no. 3, pp. 169–174, Jul. 2011.

[14] P. C. Miranda, L. Correia, R. Salvador, and P. J. Basser, "The role of tissue heterogeneity in neural stimulation by applied electric fields," *Conf Proc IEEE Eng Med Biol Soc*, vol. 2007, pp. 1715–1718, 2007.

[15] C. C. Brown, "Electroanesthesia and electrosleep.," *American Psychologist*, vol. 30, no. 3, p. 402, 1975.

[16] J. W. T. Redfearn, O. C. J. Lippold, and R. Costain, "Preliminary Account of the Clinical Effects of Polarizing the Brain in Certain Psychiatric Disorders," *The British Journal of Psychiatry*, vol. 110, no. 469, pp. 773–785, Nov. 1964.

[17] R. Costain, J. W. T. Redfearn, and O. C. J. Lippold, "A Controlled Trial of the Therapeutic Effects of Polarization of the Brain in Depressive Illness," *BJP*, vol. 110, no. 469, pp. 786–799, Nov. 1964.